

# Enhancing Two-Dimensional Electronic Spectroscopy for Layered Halide Perovskites

Sankaran Ramesh<sup>1,2,#</sup>, Minjun Feng<sup>1,#</sup>, Tomoki Furuhashi<sup>1,#</sup>, Tze Chien Sum<sup>1,\*</sup>

<sup>1</sup>Division of Physics and Applied Physics, School of Physical and Mathematical Sciences, Nanyang Technological University, 21 Nanyang Link, Singapore 637371, Singapore.

<sup>2</sup>Energy Research Institute @ NTU (ERI@N), Interdisciplinary Graduate Programme, Nanyang Technological University, 50 Nanyang Avenue, S2-B3a-01, Singapore 639798, Singapore.

# The authors contributed equally

\* Corresponding Author, Email: [Tzechien@ntu.edu.sg](mailto:Tzechien@ntu.edu.sg)

Keywords: Ruddlesden-Popper, Delocalization, Spacer Cation, Supercontinuum, Pulse Shaper, Hollow-core Fiber

## **Abstract**

The photophysics of layered halide perovskites reveals a rich disposition of exciton behaviour. Two-dimensional electronic spectroscopy (2DES) is a powerful technique for investigating such excitonic interactions and dynamics. However, the wide spectral range of layered perovskites presents a challenge in studies utilizing conventional 2DES setups to simultaneously probe their interacting excitonic states. Herein, we put forward a versatile 2DES setup employing a hollow-core fiber compressor (HCFC) to generate stable and optimized broadband laser pulses (6 fs) covering a spectral range of 500-950 nm. 2D spectra with high temporal and spectral resolution are possible even with a pulse-shaper based commercial 2DES setup. Application to a representative two-phase Ruddlesden-Popper perovskite thin film reveals well-defined signals on the diagonal and off-diagonal positions, indicative of exciton delocalization between the two transitions. Our straight-forward modification of a commercial 2DES setup extends its capabilities to investigate the large family of layered perovskites currently under intense scrutiny in the development of perovskite optoelectronics.

## **Introduction**

Two-dimensional electronic spectroscopy (2DES) is a high-resolution technique that enables the study of ultrafast dynamics in molecular systems. By measuring the sample response to a sequence of three optical pulses, it provides detailed information on the electronic structure of molecules and the coupling between electronic states.<sup>1, 2</sup> This makes 2DES a powerful tool for investigating phenomena that are challenging to study using conventional pump-probe spectroscopies. Its versatility allows for the investigation of a diverse range of molecular systems, including small molecules, complex biomolecules and light-harvesting materials,<sup>3-6</sup> exploring various phenomena such as energy transfer, electron transfer, and chemical reactions. Additionally, 2DES can provide valuable insights into interesting phenomena in semiconductors,<sup>7-10</sup> such as layered lead halide perovskites.<sup>11, 12</sup>

Layered perovskites, especially Ruddlesden-Popper (RP) perovskites, have demonstrated great promise for various applications due to their excellent optoelectronic properties. Structurally, they comprise of

alternating layers of organic molecules and inorganic lead halide octahedra, forming a distribution of quantum wells (QWs) of different thickness. Depending on the thickness ' $n$ ' of inorganic layers, they have excitonic binding energies determined by quantum and dielectric confinement effects. By careful selection of the organic molecules in the RP perovskite, their composition and optoelectronic properties can be engineered, which is advantageous in various applications such as solar cells, light-emitting diodes, photodetectors etc.<sup>13-15</sup> They also exhibit ultrafast funneling that involves transferring excitation from thinner to thicker layered phases.<sup>16, 17</sup>

Excitonic dynamics in the sub-ps timescales could be key to understanding the transfer processes in RP perovskites, yet it remains scarcely unexplored. Using 2DES, Proppe et al.<sup>18</sup> reported the exciton transfer between  $n = 2$  and  $n = 3$  phases of the order of 100 fs, which was rationalized based on QW-QW Förster theory. We showed that excitonic properties RP perovskite phases can be understood using a finite-potential QW superlattice model<sup>19</sup>, which leads to sub-ps transfer of excitons due its delocalization across layers. In a later study of mixed-phase RP perovskites using 2DES, our measurements revealed intense cross-peaks above and below the diagonal, indicating exciton delocalization across  $n = 3$  to 6 phases.<sup>20</sup> Investigating excitonic correlations among a broad range of  $n$ -phases still remains challenging as these resonances cover the visible spectrum (RP lead iodide perovskites have bandgaps between 520-800 nm). Particularly, to the best of our knowledge there are no studies investigating the inter-QW excitonic coupling and transfer among the most confined  $n = 1, 2$  phases that have much stronger excitonic confinement.<sup>21</sup> New approaches are urgently needed to enable ultrafast experiments over a wider range of excitonic resonances of layered perovskites.

To study materials such as layered perovskites that possess broad tunability of optical properties, a 2DES setup with high-quality excitation pulses and the capability to probe across the visible frequencies is highly desirable. 2DES also requires short-duration, broad band-width pulses for coherent or in-phase excitation of the transitions. Conventionally, a non-collinear optical parametric amplifier (NOPA) is used for this purpose. The working of a NOPA based on typical Ti-Sapphire amplifiers involves optical parametric amplification of a weak white light continuum pulse by an intense second harmonic of the fundamental 800 nm pulse in a birefringent crystal such as  $\beta$ -Barium Borate (BBO). To amplify the

desired modes, the geometry-dependent phase-matching conditions of the BBO must be satisfied, which generates pulses with bandwidth of a few tens of nm. The pulses generated by NOPA are typically limited by the quality of the seed white-light, the non-linear mixing crystal and the phase-matching in the crystal making pulse generation at different central frequencies challenging. Recently, HCFC has been used as an alternative broadband source for multi-dimensional spectroscopy experiments.<sup>22-24</sup> HCFC generates highly tunable supercontinuum pulses across visible frequencies through spectral broadening via self-phase modulation in a hollow fiber. Using this broadening process and the boundary conditions imposed by the fiber, they can generate pulses with bandwidths of hundreds of nm, broad spectral tunability and short pulse duration surpassing that of a NOPA. These attributes make it a useful tool to study more complex systems with multiple electronic states.

Herein, we present a new 2DES setup at our laboratory utilizing supercontinuum pulses generated by an HCFC to perform 2DES measurements in the pump-probe beam geometry. A pulse shaper is used to generate the excitation pulse pair and for choosing the excitation frequency band of interest. Using Nile Blue dye molecules as a yardstick, high-quality 2D spectra of the vibronic modulation of the electronic transition in these molecules can be obtained with our setup. We then focus on a RP perovskite thin film model system. This binary-phase RP perovskite film consists of only the  $n = 1$  and  $n = 2$  phases. Our results reveal new insights into the interaction between excitons in the two transitions, with excitons being delocalized between the  $n = 1$  and  $n = 2$  phases within a few tens of femtoseconds following excitation. This delocalization could lead to an ultrafast sub-ps funneling of excitons from higher to lower energy phases. Overall, our 2DES setup provides new capabilities to perform experiments over a broad range of energies that are relevant for the study of ultrafast phenomena in other material systems.

## **Experimental**

**2DES Setup:** The setup uses a hollow-core fiber compressor (HCFC) to generate broadband short-duration pulses as the source, and the measurements are carried out in a modified 2D visible spectrometer that has a pump-probe geometry. A schematic of our setup is shown in

**Figure 1a.** 800 nm pulses with energy 1.45 mJ at a repetition rate of 1 kHz and a pulse duration of 35 fs from a *Coherent Astrella<sup>TM</sup>* laser amplifier is employed as a seed to the HCFC (*Ultrafast Innovations*). The HCFC includes a beam stabilization unit (BSU) that contains a focusing lens and a pair of piezo-controlled mirrors to preserve the beam alignment into the 1.5 meters long hollow-core fiber. The fiber is housed inside a cylindrical chamber filled with Neon gas. The spectrally broadened pulse from the chamber enters the compressor unit that temporally compresses the pulse using 2 pairs of *PC70* chirp mirrors from *Ultrafast Innovations* and fused silica wedges to fine-tune the output pulse dispersion.

Output pulses from the HCFC are then directed to a *2DQuick Visible<sup>TM</sup>* spectrometer from *PhaseTech Spectroscopy*. The spectrometer houses an acousto-optical modulator that functions as a pulse shaper that generates the pair of excitation pulses.<sup>25</sup> To shape the optical pulse, a precisely timed radio-frequency wave is transmitted to the TeO<sub>2</sub> crystal inside the shaper. The modulator generates collinear pulse pairs that are used as pump pulses in the 2DES experiment. The window of the pulse shaper is configured to enable shaping of optical pulses up to 160 nm in bandwidth, which allows the choice of excitation band according to the sample of interest.

**Figure 1b** shows the HCFC output spectrum (black line) and the gray shaded region indicates a typical band of wavelengths that is selected by the pulse shaper. This band is broader than the bandwidth of our *Light Conversion TOPAS-White* NOPA at this range (blue, shaded region in

**Figure 1b**). A portion of the HCFC supercontinuum pulse with its full bandwidth is used as the third probe pulse.

**Figure 1a** shows the geometry of the setup where a concave mirror is used to focus both the pump and probe beams onto the sample. The angle between the pump and probe beams is minimized to reduce the dispersion and optimize time resolution of the experiment. The transmitted probe beam is directed to a *Princeton Instruments SP2150* spectrometer with an *e2v* CCD line detector.

**Preparation of Ruddlesden-popper Perovskite (RPP) thin films:** The RPP samples were fabricated in a glovebox purged with nitrogen gas. 0.2 M n-Butylammonium iodide (BAI, Greatcell Solar Materials) and 0.1 M PbI<sub>2</sub> (TCI) were mixed in DMF: DMSO (1:1 v/v) solvent and heated at 70 °C for 1 h to prepare RP1 solution. 0.2 M BAI, 0.1 M methylammonium iodide (MAI, Greatcell Solar Materials), and 0.2 M PbI<sub>2</sub> were mixed in DMF: DMSO (1:1 v/v) solvent and heated at 70 °C for 1 h to prepare RP2 solution. RP1 and RP2 precursor solutions were mixed with the volume ratio of 2:1 to obtain the final precursor solution. 10 µL of resultant precursor solution was spin coated on the glass substrate at 4,000 rpm for 30 s followed by ramping for 5 s. 20 µL of toluene was dropped 10 s after starting to spin to facilitate rapid crystallization. The coated film was annealed at 100 °C for 10 mins.

## Results

### Optimization of HCFC pulses

The HCFC output is characterized and optimized for 2DES measurements. Factors like the input pulse intensity and duration, quality of the beam and the distance of propagation in the fiber influence the supercontinuum generation by the HCFC. Furthermore, it is also sensitive to the alignment of the pump beam into the hollow-core fiber and Neon gas pressure. By ensuring optimal coupling between the beam and fiber, a transmission efficiency of 65-70% is achieved, as shown in **Figure S1**. The transmission efficiency falls at higher pressures but provides an output pulse power of > 0.90 mJ even at 2.5 bar pressure, ensuring sufficient peak power for performing 2DES experiments. At 2.2 bar absolute pressure, the output spectrum covers a broad range from 500 nm to 950 nm, as shown in

**Figure 1b**. This is the chosen configuration for our 2DES experiments. The HCFC spectra obtained at different gas pressures inside the chamber is illustrated in **Figure S2**, describing the broadening with increasing gas pressure. A typical NOPA output spectrum is shown in

**Figure 1b** to highlight the greater bandwidth obtained using the HCFC.

For an RP perovskite film with composition  $\text{BA}_2\text{MA}_3\text{Pb}_4\text{I}_{13}$ , the absorption spectrum is shown in

**Figure 1b.** The bandwidth selected by the pulse shaper from the HCFC output (gray, shaded) can excite multiple excitonic transitions of the perovskite, whereas the NOPA spectrum (blue, shaded) covers a narrower range, exciting fewer transitions in the experiment. This makes our approach suitable for the coherent spectroscopy of highly tunable semiconductors such as RP perovskites. A discussion on the comparative advantages of our method over conventional approaches is provided later in this section.

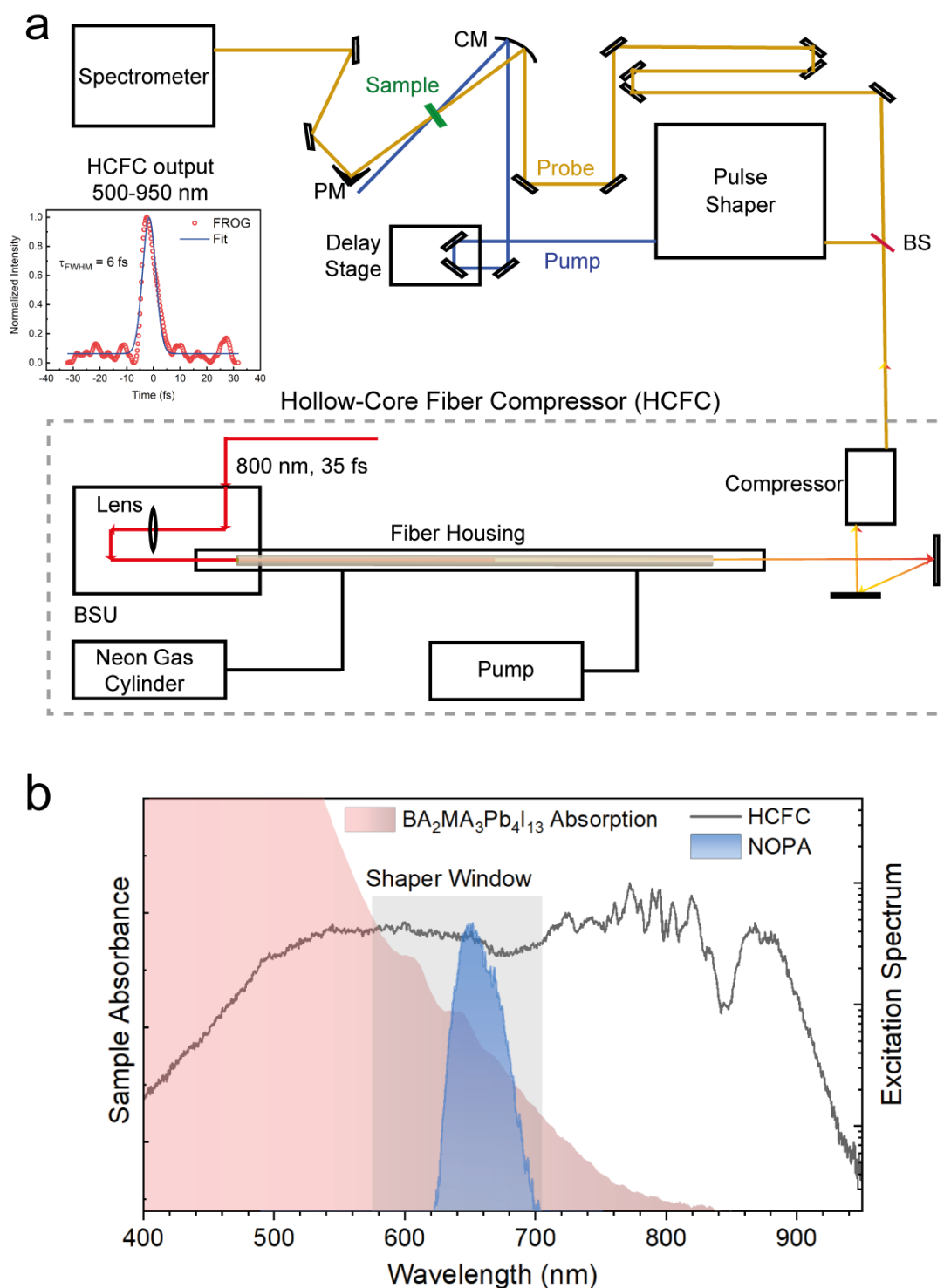


**Figure 1:** (a) Schematic of Hollow-core Fiber Compressor (HCFC) and 2DES setup. BS = beam splitter, CM = concave mirror and PM = parabolic mirror. Dotted Gray box = HCFC Setup; note that “Pump” connected to the fiber housing refers to the vacuum pump. Inset: Pulse temporal profile retrieved from a TG-FROG measurement and the Gaussian fit. HCFC output spectra (black line), (b) Absorption spectrum of  $\text{BA}_2\text{MA}_3\text{Pb}_4\text{I}_{13}$  (red, shaded) with multiple excitonic absorption peaks at 600 nm and longer wavelengths. Typical NOPA spectrum (blue, shaded) resonantly excites transitions while a typical HCFC spectrum permissible by the pulse shaper window (gray, shaded) enables one to select a broader range of excitation frequencies.

Apart from the broad spectrum, the supercontinuum pulses must also possess suitable characteristics for 2DES experiments. Particularly, the output energy must have very low and uncorrelated fluctuations to ensure that averaging over adjacent pulses yields accurate 2D spectra.<sup>26</sup> The measurement of intensity per pulse was carried out at the sample position using a *Coherent LM-150 LS* detector with a thermopile sensor, for 100,000 pulses. The stability of the HCFC output, calculated as standard deviation divided by the mean intensity was 0.8 %, similar to stabilities obtained using conventional sources such as NOPA.<sup>27</sup> The stable output pulse energy indicates that the supercontinuum output is sufficiently stable for performing time-resolved experiments. The shot-to-shot pulse energy correlation of the HCFC was also estimated based on the measurements,<sup>28, 29</sup> with the result shown in **Figure S3**. The intensity correlation between shots falls within consecutive measurements to  $< 0.2$ . The low correlation between adjacent pulses implies that the pulse energy varies mainly due to uncorrelated white noise and ensures that the measured data averaged over a fewer number of laser shots can give accurate signal convergence. These factors indicate that the HCFC output beam is ideal for performing 2DES experiments.

To ensure that the pulse is also temporally compressed, the pulse durations of the HCFC output was characterized using a home-built transient-grating frequency-resolved optical gating (FROG) setup.<sup>30</sup> The compressor unit after the fiber housing comprises of pairs of chirp mirrors and a fused silica wedge, which corrects the temporal dispersion of the broadband pulse. The optimized spectrum is processed using the FROG retrieval software to produce the pulse characteristics. The pulse duration was determined as 6 fs. The inset of

**Figure 1a** shows the retrieved temporal characteristics of the pulse. The complete characterization including the retrieved pulse spectrum is shown in **Figure S4**. The results show a nearly flat phase over the duration and spectrum of the pulse, indicating a good degree of dispersion compensation of the pulse.

We have ascertained close to transform-limited stable pulses with broad spectrum to perform 2DES experiments. These pulses are seeded into the spectrometer as described in the Experimental section. Inside the spectrometer, the beam is split into a pump and probe beam. In the experiment, the 2D signal from sample is self-heterodyned with this probe pulse. This improves the phase stability of the signal compared to BoxCARS geometry. The probe spectrum is measured over 2.50 eV to 1.76 eV.

The pump beam is then used to perform a self-diffraction FROG experiment in the spectrometer. A  $\sim 0.17$  mm-thick fused silica is used as the non-linear medium. The diffracted signal was measured at 600 nm as shown in **Figure S5**. The pulse width estimated from the FWHM of the FROG signal is  $\sim 10$  fs, indicating that short pulses are achieved after passing through the optics inside the spectrometer. This makes it possible to perform broadband pump-probe experiments with this time resolution. When the pump beam additionally passes through the pulse shaper, in which the acousto-optic wave is programmed to compensate for its own dispersion, the measured pulse is  $\sim 22$  fs (**Figure S5**). This represents the best time resolution possible in the spectrometer for 2DES experiments.

Compared to conventional methods, our approach is advantageous for the following reasons: Firstly, the excitation band is highly tunable without requiring a re-optimization of the supercontinuum source. The band is tuned via a straight-forward re-alignment of the beam into the pulse shaper. In the following sections, we will describe in detail our 2DES experiments over different excitation bands. Secondly, the pump-probe 2DES has a simpler geometry and is straightforward to implement compared to non-collinear geometries. The pulse shaper adds versatility to the setup: the pulse shaper can be programmed as a chopper to perform a 1D experiment, or it can be programmed to generate pulse pairs with tunable delay for 2D experiment. The broad probe spectrum also allows a two-color 2DES experiment, which can be used to study transitions far away in energy from the diagonal.<sup>31</sup> It is noteworthy that by modifications to the pulse shaper optics broader excitation bandwidths can be shaped, which will also raise the need for additional dispersion compensation to compress the pulses in time. Nevertheless, we have optimized the current setup without the use of any additional optical elements for dispersion compensation.

## 2DES using a pulse shaper: Nile Blue

We seek to establish the capabilities of our setup as well as resolve its spectral and temporal characteristics. Nile Blue, a common organic dye in chemical and biological applications, which is also well-studied using pump-probe spectroscopy techniques, is used as a benchmark for the first 2DES measurements. Nile blue has high absorption coefficient and coupling of a  $580\text{ cm}^{-1}$  vibrational mode to the excited electronic state.<sup>32</sup> Additionally, the dephasing time for this mode is of the order of 1 ps, which enables the observation of the clean single mode quantum beats over several cycles. Due to these reasons, Nile blue was chosen as a test system for our 2DES setup. The absorption spectrum of Nile Blue (dissolved in ethanol) is shown in **Figure 2a**. The pump spectrum used to perform 2DES measurements is overlaid on the absorption spectrum to show its overlap with the absorption peak at  $\sim 1.95\text{ eV}$ . The pump spectrum spans 1.8 eV to 2.1 eV, cropped from its original bandwidth covering 500-950 nm (

**Figure 1b**) due to the pulse shaper window.

The Nile Blue (in ethanol) is loaded in a cuvette of thickness 1 mm. The 2DES experiment was performed using shaped pulses with an average energy of  $\sim 100\text{ nJ}$  per pulse. The spot diameters of pump and probe on the sample was  $220 \pm 5\ \mu\text{m}$  and  $145 \pm 5\ \mu\text{m}$ , respectively. A broadband pump-probe scan was performed initially on the sample to locate the time-zero. For performing 2DES experiment, the coherence times  $\tau_1$  were scanned from 0 to 260 fs, with an interval of 2 fs. The waiting times  $t_2$  were scanned from -40 fs to 500 fs at intervals of 5 fs. To isolate the 2D signal from background pump-probe signals that do not have dependence on the phase of the pump pulses, a 4-frame phase-cycling scheme was implemented for the pump pulses in the scans.<sup>33</sup> The additional phases  $[\varphi_1, \varphi_2]$  to the pump pulses in each frame were :  $[\pi, 0]$ ,  $[\pi, \pi]$ ,  $[0, \pi]$ ,  $[0, 0]$ . The measurements were performed in a rotating frame at 714 nm. The 2D maps are generated by performing Fourier transform of the data over  $\tau_1$  values to obtain the excitation or pump energy axis, while the detection using the spectrometer directly provides the spectra along the emission or probe energy axis.

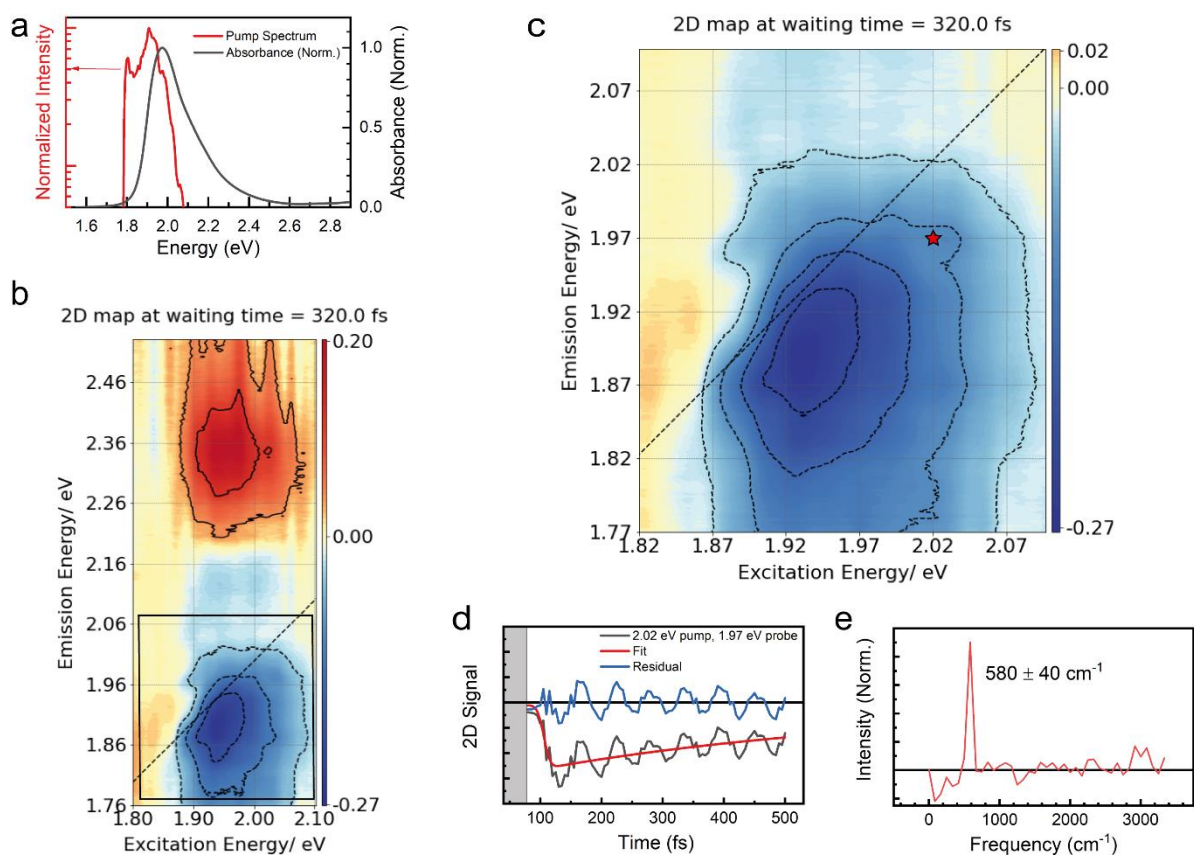


**Figure 2:** 2DES Experiments on Nile Blue in ethanol solution (a) Absorption spectrum of Nile blue (black line) and the pump spectrum used for 2DES experiment (red line) (b) 2D spectrum at waiting time  $t_2 = 320$  fs. Area within black square of (b) is replotted in (c). (d) Kinetics at pump energy 2.03 eV and probe energy 1.97 eV (black line, the position on 2D map marked in (c) with red star). The dynamics is fitted with a mono-exponential decay function (red line). Blue curve shows the residual of the fit. (e) Fourier transform of the residual signal shown in (d).

**Figure 2b** shows the 2D spectrum of the Nile Blue in ethanol solution at a waiting time of  $t_2 = 320$  fs. 2D spectra at different waiting times with complete emission energy axes are given in **Figure S6**. The emission energy axis is shown for the range of 2.50 eV to 1.76 eV. The 2D spectrum shows a broad negative signal centered at  $\sim 1.9$  eV emission energy. The positive signal at  $\sim 2.36$  eV emission energy is the excited state absorption signal of Nile Blue. In **Figure 2c**, the emission energy axis of the spectrum in **Figure 2b** has been cropped to study the negative signal. The spectrum shows an elongated lineshape due to inhomogeneous broadening and the excitation of its multiple vibrational modes due to vibronic coupling.<sup>34</sup> The excitation spectrum near the band edge ensures minor contributions of hot carrier relaxation effects. Further, the peak lies below the diagonal, shifted to lower energy along the emission energy axis due to the contribution from stimulated emission. The non-linear signal comprises of a

combination of ground-state bleach and the red-shifted stimulated emission signal, both of which are emitted in the same direction in our experiment. Therefore, these contributions add up, resulting in a shift of the peak to a lower energy.<sup>23, 35</sup>

The bleach signal was studied across waiting times to study the photoinduced dynamics. Signal on positions on 2D signal maps across waiting times were analyzed and vibrational modulation of the dynamics was observed over a region of the 2D map. The dynamics is depicted in **Figure 2c**, which shows the temporal dynamics at a pump energy 2.02 eV and probe energy of 1.97 eV. The dynamics at additional points covering the region of vibrational modulation is shown in **Figure S7**. The early part of the dynamics (in the shaded gray region in **Figure 2c**) has been omitted here since it contains artefacts at the early waiting times. The assumption used in interpreting 2D signals is that the light pulses are described by  $\delta$ -functions, which simplifies the different signal pathways related to the third-order non-linear signal. This assumption is reasonable at longer waiting times  $t_2$ , whereas at the early times when the light pulses of finite duration overlap, it can lead to undesirable signals from incorrect pulse ordering. Such unwanted signals or artefacts distort the lineshapes and dynamics. Further sources of artefacts include the spectral chirp and imperfect pump and probe pulse profiles interfering with the 2D signals.<sup>36, 37</sup> In general, 2D spectra at waiting times within twice the excitation pulse duration are affected, therefore, we consider the 2D spectra well beyond this limit (here we chose 2D maps at  $t_2 > 70$  fs, while the time resolution is 22 fs). The dynamics shown in **Figure 2c** is fitted using an exponential decay function (red curve) and the residual of the fitting (blue curve) contains purely the oscillatory part of the observed signal. The Fourier transform of the residual is shown in **Figure 2d**, providing a spectrum of the oscillatory modes. The spectrum shows a peak at the frequency of  $580\text{ cm}^{-1}$ , corresponding to a period of  $\sim 57$  fs. The modulation can be attributed to the Franck-Condon vibrational states associated with the electronic transition excited by the short duration laser pulse. The observed mode originates from the ring-distortion mode of Nile Blue that is widely reported.<sup>32</sup> It is worth noting that the  $880\text{ cm}^{-1}$  vibrational mode of the ethanol solvent is not expected to be observed in the experiment, since only the Franck-Condon coupled modes to the excited electronic state of Nile Blue are excited in the experiment. The ability to resolve these vibronic beats shows that

our setup can perform 2DES experiments with high spectral and temporal resolution. Next, we turn our attention to test the system with model binary-phase RP perovskite thin film sample, whose excitonic peaks are located close to the edge of the HCFC supercontinuum.

## 2DES of Binary Phase RP Perovskite Film

Here, we focus on the characterization of an archetypal binary-phase RP perovskite thin film with  $n = 1$  and  $n = 2$  phases as a further test of the setup to measure over different energy bands simply by modulating the pulse shaper. As described previously, quantum wells (QW) with different thicknesses (or  $n$ -phases) are formed in RP perovskite films. Band alignments between the  $n$ -phases are modulated due to quantum and dielectric confinement effects, producing a system with wide variations in its electronic structure. Excitons in this system exhibit ultrafast dynamics where they localize from higher bandgap (low- $n$ ) to lower bandgap (high- $n$ ) phases. The timescale of the ultrafast exciton transfer has been predicted to be in the sub-ps timescale and probably includes strong coupling of inter-QW exciton states.<sup>20, 21</sup> Giovanni *et al.* performed pump-probe measurements with different excitation energies to decipher the interaction between  $n$ -phases in a mixed-phase RP perovskite film.<sup>19</sup> The study revealed that a sub-ps localization is involved mediated by wavefunction delocalization across QWs. However, experimentally resolving such process as well as studying the coupling between individual  $n$ -phases remain challenging using pump-probe spectroscopy.

In the 2DES experiment, the broadband pump coherently excites multiple  $n$ -phases within its spectral bandwidth. 2DES measurements on RP films have been reported on films containing many (typically more than 4)  $n$ -phases. In such samples, complicated 2D maps with multiple resonances are obtained. To clarify the ultrafast dynamics between one pair of adjacent  $n$ -phases, we introduce RP perovskite films where the  $n$ -phases are restricted to thicknesses of  $n = 1$  and 2 only, as a model system for investigation of the interactions among excitons in the thinnest phases (largest wavefunction delocalization<sup>19</sup>). A schematic of the film structure is shown in **Figure 3a**. The synthesis of the film is described in the experimental section. **Figure 3b** shows the linear absorption spectrum of the sample

used for measurement. The spectrum comprises of two sharp peaks that originate from the excitonic absorption in the  $n = 1$  and  $n = 2$  phases at energies  $\sim 2.40$  eV and  $\sim 2.20$  eV, respectively. The spectrum of the excitation laser pulses is overlaid on the absorption spectrum in **Figure 3b**. For this experiment, the pump spectrum is shifted towards the 2.45 eV – 2.10 eV band by simply shifting the alignment of the broadband pump beam with the pulse shaper module. With this spectrum, we perform 2D experiments coherently exciting the  $n = 1$  and 2 phases. This capability of our setup allows greater freedom to set up the experiment for different sample or different electronic states, avoiding the need for complex realignment of the supercontinuum source.

For the 2D experiment, the coherence time was scanned from 0 to 300 fs at intervals of 2 fs. The waiting times  $t_2$  were scanned from 0 fs to 1000 fs at intervals of 5 fs until 180 fs and at every 10 fs from 180 fs upto 1000 fs. 4-frame phase-cycling of the pump pulses was performed in the same way as was described for the experiments on the Nile Blue solution. The measurements were performed in a rotating frame at 606 nm. **Figure 3c** shows the 2D map of the RP perovskite film at  $t_2 = 100$  fs. The emission energy axis of the spectrum has been cropped from the complete 2D map we obtained in order to show the region of interest. 2D spectra at later waiting times with complete emission energy axis is shown in **Figure S8**. There are two photobleaching peaks along the diagonal arising from the two discrete excitonic states in the sample. The diagonal signals at  $\sim 2.38$  eV and  $\sim 2.19$  eV indicate the population of excitons in the  $n = 1$  and  $n = 2$  phases, respectively. At the on-diagonal positions on the map, the signal is elongated along the diagonal due to the inhomogeneous broadening due to structural disorder of the phases in the sample. At later waiting times, the peaks attain a more symmetrical shape due to spectral diffusion. The signal at the  $n = 2$  phase diagonal is elongated along the excitation energy axis. This indicates the energetic distribution of thermalized excitons in the  $n = 2$  phase.<sup>8</sup> The well-defined peaks along the diagonal indicate the absence of any intermediate states between the two transitions.<sup>20</sup> The excitons in higher energy  $n = 1$  phase could transfer to the lower energy  $n = 2$  phase, for which we next examine the temporal evolution of the 2D spectra.

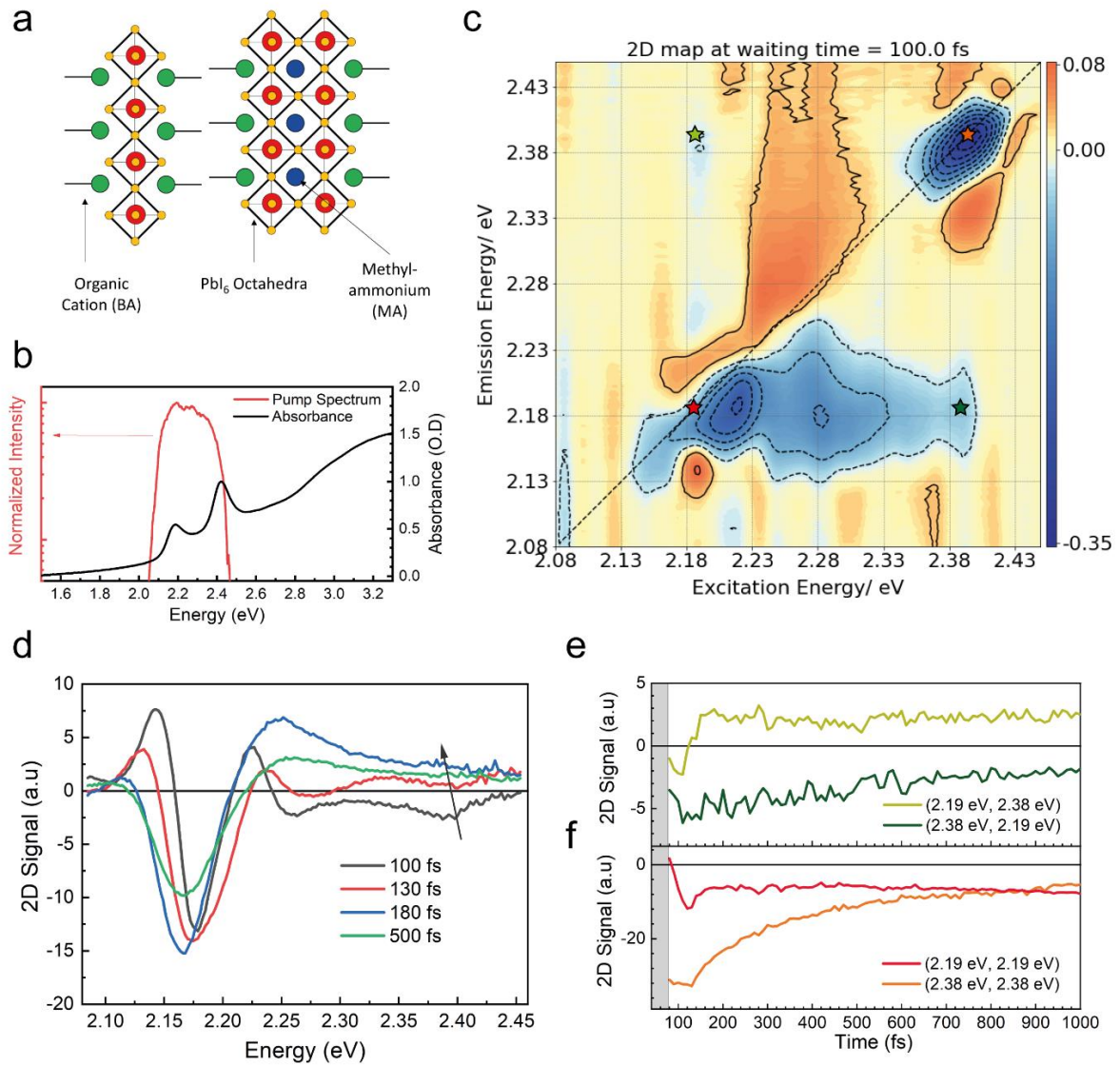


**Figure 3:** 2DES experiment on RP perovskite film. (a) Schematic of structure of binary-phase RP perovskite, showing  $n = 1$  and  $n = 2$  phases separated by organic spacer molecules. (b) Absorption spectrum of RP perovskite film (black line) and the pump spectrum used for 2DES experiment (red line). (c) 2D spectrum of the RP perovskite film at  $t_2 = 100$  fs. The spectrum is marked at on-diagonal and off-diagonal positions, the kinetics at these positions are shown in (e-f). (d) pseudo-TA spectra or the vertical slice of the 2D spectra at different waiting times, at the excitation energy of 2.19 eV. Black arrow shows the short-lived signal at the above-diagonal cross-peak. (e-f) Kinetics of the 2D signal at the cross peaks (e) and on-diagonal peaks (f). The corresponding positions are indicated in the figure legend according to their respective (excitation energy, emission energy).

This 2D map at early waiting time reveals insights into the ultrafast processes in the binary RP perovskite. The coupling between these excitonic states can be studied by monitoring the cross peaks, one above the diagonal on the map with respective excitation and emission energy at (2.19 eV, 2.38 eV), and one below the diagonal with the energies (2.38 eV, 2.19 eV) respectively. At the waiting time of 100 fs, a signal can be observed at both the above-diagonal and below-diagonal cross-peaks, as shown in **Figure 3c**. The appearance of cross-peaks between the two transitions implies the presence of strong excitonic coupling between them. Such response has been reported between transitions that share a common electronic state, for example a shared eigenstate.<sup>5, 10, 38</sup> Here, this results from a delocalization of the excitation between the two transitions due to the organic spacers acting as finite potential barriers.<sup>19</sup>

Next, we examine the evolution of slices of the 2D spectra at a specific excitation energy, referred to as the pseudo-transient absorption (pseudo-TA) spectrum. These are obtained from vertical cuts of the 2D-maps, which is analogous to a TA spectrum with a narrowband excitation centred at the chosen excitation energy. **Figure 3d** shows such pseudo-TA spectrum at the excitation energy of 2.19 eV, corresponding to the  $n = 2$  exciton transition. The peak at 2.38 eV in **Figure 3d** corresponding to the above-diagonal cross-peak is evident at early waiting times. At later waiting times, the cross-peak disappears as indicated by the black arrow. To analyze the dynamics in detail, the kinetics at cross-peaks on the 2D map are plotted as shown in **Figure 3e**. The colour scheme in **Figure 3e** corresponds to that of the marked points on the 2D map (**Figure 3c**). Data at  $t_2 < 80$  fs is omitted here for similar reasons as in the case of Nile Blue: in this early regime the effects of incorrect pulse ordering distort the spectra, making the data unreliable. However, even at early waiting times studied here (where  $t_2 < 120$  fs) cross-peaks above and below the diagonal are clearly visible. The above-diagonal cross-peak signal decays at later waiting times  $t_2 > 120$  fs (data in the lime-green curve, **Figure 3e**), indicating that the delocalization between the two transitions is short-lived. The cross-peak observed in the 2D spectra at early waiting times are an indication of coupling of the  $n = 1$  and  $n = 2$  transitions via wavefunction delocalization. Such delocalization existing at sub-ps timescales could be a precursor to ultrafast funnelling of excitons. The below-diagonal cross-peak also decays (olive green curve), albeit

at a slower rate. Similar decay is also observed for the on-diagonal signals shown in **Figure 3f**. The slower overall decay of signals at different points on the 2D spectra could be attributed to the recombination of excitons leading to the reduction of the photobleaching.

The measurement outcomes agree with our previous results,<sup>20</sup> where a delocalization of excitation was characterized in a mixed-phase RP perovskite film using a BoxCARS 2DES setup. While these results show the capability of our 2DES setup to generate excellent 2DES data, they also underline the universality of exciton delocalization in RP perovskite films. We posit that such delocalization plays a role in ultrafast exciton funnelling from low- $n$  to high- $n$  phases. Tailoring the interlayer coupling by using organic cations or ligands that provide a weaker barrier or by tailoring the structural disorder of the phases may reveal stronger cross-peaks, and in turn also be useful for manipulating exciton transport in these layered systems.<sup>39</sup>

## Conclusion

In this work, we present a novel 2D electronic spectroscopy (2DES) setup in pump probe geometry that utilizes a hollow-core fiber compressor (HCFC) as the broadband light source. This HCFC approach is shown to be a versatile and efficient method for generating high-quality supercontinuum pulses, ranging from 500 – 950 nm. We adapt a commercially available 2DES spectrometers for studying the highly tunable layered halide perovskites. By coupling to a pulse shaper, we select the excitation band as required for the experiment by optimizing the alignment between HCFC pulses and the pulse shaper, enabling the straight-forward acquisition of absorptive 2D spectra of different samples. Through our preliminary experiments using this setup, we demonstrate its potential in providing valuable insights into the ultrafast dynamics of complex molecular systems, particularly layered halide perovskites. Our first experiment with the Nile Blue dye reveals the exceptional quality and resolution of data generated by our setup. The capability of our setup for studying excitonic resonances over a broad spectral range is confirmed by our results that reveal for the first time the excitonic coupling between  $n = 1$  and  $n = 2$  phases of an RP perovskite film. Overall, our findings suggest that this setup is an invaluable tool for

investigating and manipulating the excitonic coupling in halide perovskites, especially in highly ordered systems such as perovskite superlattices<sup>40</sup> thereby facilitating their development of perovskite materials for optoelectronic applications.

### **Supporting Information**

The Supporting Information is available free of charge at .

HCFC properties at different neon gas pressures; HCFC pulse-to-pulse energy correlation; Pulse retrieval using FROG; 2DES of Nile Blue in ethanol; 2DES of RP perovskite film (PDF)

### **Conflict of Interest**

The authors declare no conflict of interest.

### **Data Availability Statement**

The data that support the findings of this study are openly available in DR-NTU (Data) at <https://doi.org/10.21979/N9/41FE8K>.

### **Funding Sources**

This research is supported by the Ministry of Education, Singapore, under its AcRF Tier 2 grant (MOE-T2EP50120-0004) and the National Research Foundation, Singapore (NRF) under its NRF Investigatorship (NRF-NRFI2018-04) and the Competitive Research Programme (NRF-CRP25-2020-0004).

Received: ((will be filled in by the editorial staff))

Revised: ((will be filled in by the editorial staff))

Published online: ((will be filled in by the editorial staff))

### **References**

- (1) Jonas, D. M. Two-dimensional femtosecond spectroscopy. *Annual review of physical chemistry* **2003**, *54* (1), 425-463.
- (2) Cho, M. Coherent two-dimensional optical spectroscopy. *Chemical reviews* **2008**, *108* (4), 1331-1418.

- (3) Harel, E.; Engel, G. S. Quantum coherence spectroscopy reveals complex dynamics in bacterial light-harvesting complex 2 (LH2). *Proceedings of the National Academy of Sciences* **2012**, *109* (3), 706-711.
- (4) Dostál, J.; Pšenčík, J.; Zigmantas, D. In situ mapping of the energy flow through the entire photosynthetic apparatus. *Nature Chemistry* **2016**, *8* (7), 705-710.
- (5) Cassette, E.; Dean, J. C.; Scholes, G. D. Two - Dimensional Visible Spectroscopy For Studying Colloidal Semiconductor Nanocrystals. *Small* **2016**, *12* (16), 2234-2244.
- (6) Lott, G. A.; Perdomo-Ortiz, A.; Utterback, J. K.; Widom, J. R.; Aspuru-Guzik, A.; Marcus, A. H. Conformation of self-assembled porphyrin dimers in liposome vesicles by phase-modulation 2D fluorescence spectroscopy. *Proceedings of the National Academy of Sciences* **2011**, *108* (40), 16521-16526.
- (7) Cassette, E.; Pensack, R. D.; Mahler, B.; Scholes, G. D. Room-temperature exciton coherence and dephasing in two-dimensional nanostructures. *Nature communications* **2015**, *6* (1), 6086.
- (8) Richter, J. M.; Branchi, F.; Valduga de Almeida Camargo, F.; Zhao, B.; Friend, R. H.; Cerullo, G.; Deschler, F. Ultrafast carrier thermalization in lead iodide perovskite probed with two-dimensional electronic spectroscopy. *Nature communications* **2017**, *8* (1), 376.
- (9) Yu, B.; Chen, L.; Qu, Z.; Zhang, C.; Qin, Z.; Wang, X.; Xiao, M. Size-dependent hot carrier dynamics in perovskite nanocrystals revealed by two-dimensional electronic spectroscopy. *The Journal of Physical Chemistry Letters* **2020**, *12* (1), 238-244.
- (10) Cassette, E.; Pedetti, S.; Mahler, B.; Ithurria, S.; Dubertret, B.; Scholes, G. Ultrafast exciton dynamics in 2D in-plane hetero-nanostructures: delocalization and charge transfer. *Physical Chemistry Chemical Physics* **2017**, *19* (12), 8373-8379.
- (11) Yuan, M.; Quan, L. N.; Comin, R.; Walters, G.; Sabatini, R.; Voznyy, O.; Hoogland, S.; Zhao, Y.; Beauregard, E. M.; Kanjanaboos, P. Perovskite energy funnels for efficient light-emitting diodes. *Nature nanotechnology* **2016**, *11* (10), 872-877.
- (12) Fu, J.; Ramesh, S.; Melvin Lim, J. W.; Sum, T. C. Carriers, Quasi-particles, and Collective Excitations in Halide Perovskites. *Chemical Reviews* **2023**, *123* (13), 8154-8231.
- (13) Chen, Y.; Sun, Y.; Peng, J.; Tang, J.; Zheng, K.; Liang, Z. 2D Ruddlesden–Popper perovskites for optoelectronics. *Advanced Materials* **2018**, *30* (2), 1703487.
- (14) Qing, J.; Ramesh, S.; Xu, Q.; Liu, X. K.; Wang, H.; Yuan, Z.; Chen, Z.; Hou, L.; Sum, T. C.; Gao, F. Spacer Cation Alloying in Ruddlesden–Popper Perovskites for Efficient Red Light - Emitting Diodes with Precisely Tunable Wavelengths. *Advanced Materials* **2021**, *33* (49), 2104381.
- (15) Liang, C.; Gu, H.; Xia, Y.; Wang, Z.; Liu, X.; Xia, J.; Zuo, S.; Hu, Y.; Gao, X.; Hui, W. Two-dimensional Ruddlesden–Popper layered perovskite solar cells based on phase-pure thin films. *Nature Energy* **2021**, *6* (1), 38-45.
- (16) Grancini, G.; Nazeeruddin, M. K. Dimensional tailoring of hybrid perovskites for photovoltaics. *Nature Reviews Materials* **2019**, *4* (1), 4-22.
- (17) Righetto, M.; Giovanni, D.; Lim, S. S.; Sum, T. C. The photophysics of Ruddlesden–Popper perovskites: A tale of energy, charges, and spins. *Applied Physics Reviews* **2021**, *8* (1), 011318.
- (18) Proppe, A. H.; Elkins, M. H.; Voznyy, O.; Pensack, R. D.; Zapata, F.; Besteiro, L. V.; Quan, L. N.; Quintero-Bermudez, R.; Todorovic, P.; Kelley, S. O. Spectrally resolved ultrafast exciton transfer in mixed perovskite quantum wells. *The journal of physical chemistry letters* **2019**, *10* (3), 419-426.
- (19) Giovanni, D.; Ramesh, S.; Righetto, M.; Melvin Lim, J. W.; Zhang, Q.; Wang, Y.; Ye, S.; Xu, Q.; Mathews, N.; Sum, T. C. The physics of interlayer exciton delocalization in Ruddlesden–Popper lead halide perovskites. *Nano Letters* **2020**, *21* (1), 405-413.
- (20) Ramesh, S.; Giovanni, D.; Righetto, M.; Ye, S.; Fresch, E.; Wang, Y.; Collini, E.; Mathews, N.; Sum, T. C. Tailoring the Energy Manifold of Quasi - Two - Dimensional Perovskites for Efficient Carrier Extraction. *Advanced Energy Materials* **2022**, *12* (10), 2103556.

- (21) Elkins, M. H.; Pensack, R.; Proppe, A. H.; Voznyy, O.; Quan, L. N.; Kelley, S. O.; Sargent, E. H.; Scholes, G. D. Biexciton resonances reveal exciton localization in stacked perovskite quantum wells. *The Journal of physical chemistry letters* **2017**, *8* (16), 3895-3901.
- (22) Ma, X.; Dostál, J.; Brixner, T. Broadband 7-fs diffractive-optic-based 2D electronic spectroscopy using hollow-core fiber compression. *Optics Express* **2016**, *24* (18), 20781-20791.
- (23) Mewes, L.; Ingle, R. A.; Al Haddad, A.; Chergui, M. Broadband visible two-dimensional spectroscopy of molecular dyes. *The Journal of Chemical Physics* **2021**, *155* (3), 034201.
- (24) Sonnichsen, C.; Brosseau, P.; Reid, C.; Kambhampati, P. OPA-driven hollow-core fiber as a tunable, broadband source for coherent multidimensional spectroscopy. *Optics Express* **2021**, *29* (18), 28352-28358.
- (25) Middleton, C. T.; Woys, A. M.; Mukherjee, S. S.; Zanni, M. T. Residue-specific structural kinetics of proteins through the union of isotope labeling, mid-IR pulse shaping, and coherent 2D IR spectroscopy. *Methods* **2010**, *52* (1), 12-22.
- (26) Turner, D. B. Standardized specifications of 2D optical spectrometers. *Results in Chemistry* **2019**, *1*, 100001.
- (27) Brazard, J.; Bizimana, L. A.; Turner, D. B. Accurate convergence of transient-absorption spectra using pulsed lasers. *Review of Scientific Instruments* **2015**, *86* (5), 053106.
- (28) Polli, D.; Lüer, L.; Cerullo, G. High-time-resolution pump-probe system with broadband detection for the study of time-domain vibrational dynamics. *Review of Scientific Instruments* **2007**, *78* (10), 103108.
- (29) Schrieffer, C.; Lochbrunner, S.; Riedle, E.; Nesbitt, D. Ultrasensitive ultraviolet-visible 20 fs absorption spectroscopy of low vapor pressure molecules in the gas phase. *Review of Scientific Instruments* **2008**, *79* (1), 013107.
- (30) Trebino, R.; DeLong, K. W.; Fittinghoff, D. N.; Sweetser, J. N.; Krumbügel, M. A.; Richman, B. A.; Kane, D. J. Measuring ultrashort laser pulses in the time-frequency domain using frequency-resolved optical gating. *Review of Scientific Instruments* **1997**, *68* (9), 3277-3295.
- (31) Myers, J. A.; Lewis, K. L.; Tekavec, P. F.; Ogilvie, J. P. Two-color two-dimensional Fourier transform electronic spectroscopy with a pulse-shaper. *Optics express* **2008**, *16* (22), 17420-17428.
- (32) Fragnito, H.; Bigot, J.-Y.; Becker, P.; Shank, C. Evolution of the vibronic absorption spectrum in a molecule following impulsive excitation with a 6 fs optical pulse. *Chemical Physics Letters* **1989**, *160* (2), 101-104.
- (33) Zhang, Z.; Wells, K. L.; Hyland, E. W. J.; Tan, H.-S. Phase-cycling schemes for pump-probe beam geometry two-dimensional electronic spectroscopy. *Chemical Physics Letters* **2012**, *550*, 156-161.
- (34) Lawless, M. K.; Mathies, R. A. Excited state structure and electronic dephasing time of Nile blue from absolute resonance Raman intensities. *The Journal of chemical physics* **1992**, *96* (11), 8037-8045.
- (35) Brixner, T.; Mančal, T.; Stiopkin, I. V.; Fleming, G. R. Phase-stabilized two-dimensional electronic spectroscopy. *The Journal of chemical physics* **2004**, *121* (9), 4221-4236.
- (36) Yetzbacher, M. K.; Belabas, N.; Kitney, K. A.; Jonas, D. M. Propagation, beam geometry, and detection distortions of peak shapes in two-dimensional Fourier transform spectra. *The Journal of chemical physics* **2007**, *126* (4), 044511.
- (37) Paleček, D.; Edlund, P.; Gustavsson, E.; Westenhoff, S.; Zigmantas, D. Potential pitfalls of the early-time dynamics in two-dimensional electronic spectroscopy. *The Journal of Chemical Physics* **2019**, *151* (2), 024201.
- (38) Righetto, M.; Bolzonello, L.; Volpato, A.; Amoroso, G.; Panniello, A.; Fanizza, E.; Striccoli, M.; Collini, E. Deciphering hot-and multi-exciton dynamics in core-shell QDs by 2D electronic spectroscopies. *Physical Chemistry Chemical Physics* **2018**, *20* (27), 18176-18183.
- (39) Boeije, Y.; Van Gompel, W. T.; Zhang, Y.; Ghosh, P.; Zelewski, S. J.; Maufort, A.; Roose, B.; Ooi, Z. Y.; Chowdhury, R.; Devroey, I. Tailoring Interlayer Charge Transfer Dynamics in 2D Perovskites with Electroactive Spacer Molecules. *Journal of the American Chemical Society* **2023**, *145* (39), 21330-21343.

(40) Lei, Y.; Li, Y.; Lu, C.; Yan, Q.; Wu, Y.; Babbe, F.; Gong, H.; Zhang, S.; Zhou, J.; Wang, R. Perovskite superlattices with efficient carrier dynamics. *Nature* **2022**, *608* (7922), 317-323.

TOC Graphic:

